Research Square

Preprints are preliminary reports that have not undergone peer review.
They should not be considered conclusive, used to inform clinical practice,
or referenced by the media as validated information.

The Retinex Enhancement Algorithm for Low-light Intensity Image Based on Improved Illumination Map

Ruidi Weng
Zhejiang Normal University
Ya Zhang
Zhejiang Normal University
Hanyang Wu
wuhanyang@zjnu.edu.cn
Zhejiang Normal University
Weiyong Wang
Zhejiang Jinfei Machinery Co.LTD
Dongyun Wang
Zhejiang Normal University

Research Article

Keywords: Low-light enhancement, Retinex, Nonlinear Gamma correction, Image fusion

Posted Date: March 7th, 2024

DOI: https://doi.org/10.21203/rs.3.rs-4011872/v1

License: This work is licensed under a Creative Commons Attribution 4.0 International License.
Read Full License

Additional Declarations: No competing interests reported.

The Retinex Enhancement Algorithm for Low-light Intensity Image Based on Improved Illumination Map

Ruidi Weng[1], Ya Zhang[1], Hanyang Wu*[1], Weiyong Wang[2], Dongyun Wang*[1]

[1] Zhejiang Provincial Key Laboratory of Urban Rail Transit Intelligent Operation and Maintenance Technology and Equipment, Zhejiang Normal University, Zhejiang 321005, China

[2] Zhejiang Jinfei Machinery Co.LTD, Zhejiang ,321004,China.

***Corresponding author:** wuhanyang@zjnu.edu.cn, zsdwdy@zjnu.edu.cn

Abstract: Due to the low brightness of the images taken in low-light intensity conditions, the image processing precision will be affected. In this paper, the Gamma Function based on the brightness average and the weighted fusion method according to gray entropy are proposed. They are combined with the improved Retinex algorithm. Firstly, the maximum values of R, G, and B channels in the original image are extracted to form the primary illumination map. Secondly, the illumination map is optimized by the optimization problems and adjusted by using the Gamma correction function based on the average brightness value. Finally, the illumination map and detail layer are fused by a weighted fusion algorithm of gray entropy to obtain the reflection map. Reflection maps are used as enhancement results. The algorithm proposed in this paper can improve the brightness and can maintain light distribution in the original image and has less color distortion.

Keywords: Low-light enhancement; Retinex; Nonlinear Gamma correction; Image fusion

1. Introduction

For images taken in low-light intensity conditions, the quality can be very poor due to considerable noise [1]. These phenomena occur in many machine vision-based tasks such as underwater object detection [2], medical imaging technology [3], and fault detection [4]. It is great significance to develop a low-light image enhancement algorithm for extending machine vision applications.

The grayscale of low-light images is in a limited area with a small average value. Stretching the grayscale to a large area may be the most intuitive algorithm, such as histogram equalization [5][6]. The Control Limited Adaptive Histogram Equalization (CLAHE) [5] is a strategy based on HE that deals with the problem of excessive contrast by cropping histograms. Further, Dynamic Histogram Equalization (DHE) method [6] attempts segmentation of the histogram after smoothing it. However, this method can lead to noise, loss of detail, or overexposure with the image contrast is increased. A second type of intuitive solution is the Gamma Correction (GC) algorithm. Precisely, the GC dynamically adjusts each pixel based on specified characteristics, such as the degree to which it deviates from the mean gray level or the brightness of the current location in the corresponding illumination map. The drawback is that it didn't consider the relationship between pixels on the structure or edge, resulting in limited contrast image enhancement.

The Retinex theorem [7], which simulates human vision mechanisms, suggests that an image can be decomposed into the reflectance and illumination map. Based on Retinex, Several methods have been developed to estimate illumination maps or compensate for reflectance contrast efficiently. The original single-scale Retinex algorithm (SSR) [8] and multi-scale Retinex (MSR) [9]methods use local Gaussian filtering to estimate illumination maps. The subsequent researchers tried to use the center-surrounding algorithms to enhance the illumination map which was recognized to retain more edges and structure. Zhang et al. [10] used the enhanced double-pass fast filtering to estimate the illumination map. Yu et al. [11], and Xue Yang et al. [12] used the guided filtering to estimate the illumination map of the images. Due to the non-smoothness of the illumination map, the texture coherence between the enhancement image and the original image is subject to deviation. Guo et al. [13] proposed a method of image enhancement that reveals structure at low illumination levels. It improved both the brightness and the contrast. Guo et al. [13], and Zhang et al. [14] overcame the overexposed state by adding image inversion and fusion stages. However, in this method, the detailed changes in illumination after the gradient domain constraints are not considered. This results in localized overexposure and under-enhancement of low-light areas in the enhanced image. For the problem of structural texture consistency, Xu et al. [15] proposed using a structure and texture aware retinex model (STAR) to process multiple types of images at a time. Xu et al. [16] proposed a novel multi-scale fusion framework for low-illumination image enhancement, this method uses a remapping function in order to generate multiple exposure images and selects the fused features as weight maps, and finally introduces a pyramid fusion scheme for fusion, which can effectively maintain the details and color information of the images.

Deep learning has been applied to Retinex in recent years as well. Zhang et al. [17] carried out the decomposition and enhancement of reflectance and illumination using convolutional neural networks based on the theory of Retinex. Zhang et al. [18] proposed a training method using matched images with different exposure conditions. Li et al. [19] designed a gradient-guided low-illumination enhancement network containing enhancement branch and gradient branch, where the enhancement branch learn under the guidance

of the gradient branches, and designed an attention graph-based distillation loss to transfer knowledge, which can be done to retain more image details. Wang et al. [20] proposed an adaptive single-image enhancement framework that combines a virtual exposure strategy with image fusion, and this approach mitigates the problems of local under/overenhancement of the enhanced image as well as the lack of robustness of parameter settings. While deep learning can quickly improve the contrast and brightness of a large numbers of images, it still has the problem of inaccurate color reproduction.

This paper proposes an enhanced Retinex method and a gamma function based on the average brightness value and a method for fusing the detail layer according to the gray entropy. Constrained by the gradient term, some regional pixels have a smaller gray value than the initial illumination map after the optimization problem. Therefore, using the optimized illumination map is prone to overexposure of the reflection map. Previous literatures [13][22][23] have attempted to address this problem by adjusting the brightness of the illumination maps using gamma functions. When the average brightness is different, the illuminance needs to be increased to a different value. This paper proposes a gamma function based on the average brightness to correct the illumination map to overcome this problem. In addition, the detail layer is added to the final illumination according to the proposed weighting strategy. Experiments were conducted for different challenging images to demonstrate the effectiveness of our method.

2. Algorithm Principles

Fig. 1 shows a flowchart of the system. Firstly, the maximum value of R, G, and B channels is extracted as the initial illumination map's brightness value, and guided filtering is applied to the illumination map. Once the filtered map is obtained, it is optimized by combining local coherence and alternating minimization. Then, the optimized illumination is adjusted by the nonlinear gamma function. Finally, a detail layer is added to the adjusted illumination by weighting. The detail layer is obtained by the difference between the original image and the original image with the Gaussian filter. The weight is the difference between the gray entropy of the original illumination map and the optimized illumination map.

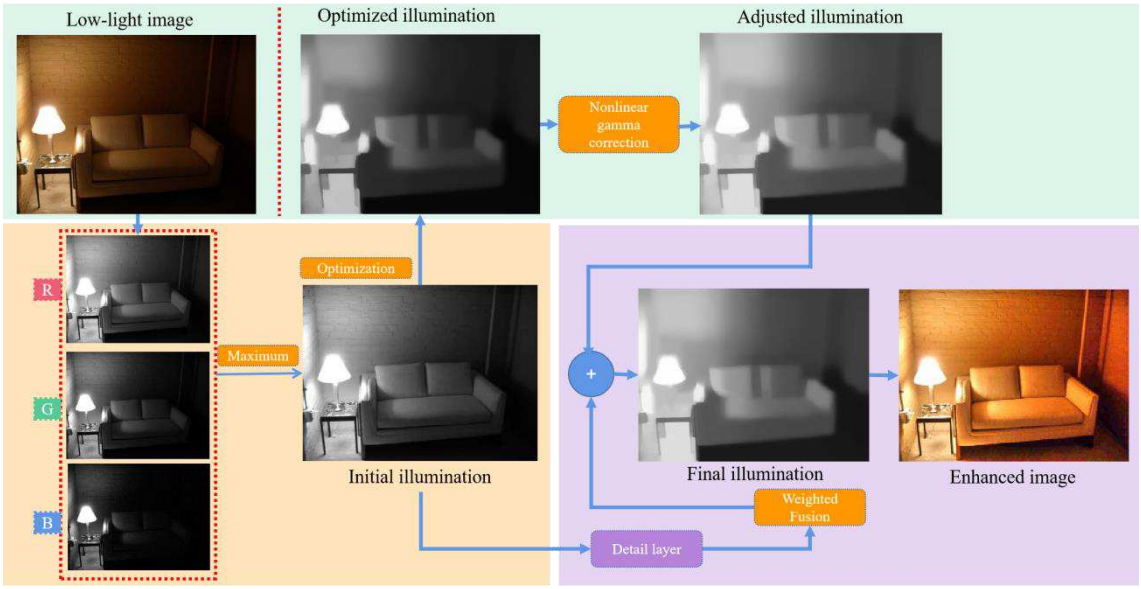


Fig. 1. Flowchart of the system.

2.1Retinex Theory

The proposed algorithm assumes that the images viewed by the human eyes consist of reflectance and illumination components such as equation **(1)**:

$$I=R\circ T \tag{1}$$

where I represents the original figure, R represents the reflection component, T represents the illumination component, and the operator $\circ$ represents the multiplication of pixels by pixels. In the usual methods, the illumination component is estimated in the log domain. Then, the reflection component is restored. Finally, the reflection component is used as an enhanced image such as equation **(2)**:

$$\log R(x,y)=\log I(x,y)-\log T(x,y) \tag{2}$$

where x and y denote the image abscissa and ordinate respectively. Methods for estimating reflection in the logarithmic domain ignore image reflectivity requirements [7]. In recent years, researchers have proposed to merge the reflection map with the optimized illumination map in the linear domain. This method uses the combined result as the enhancement map. In this paper, we use the reflection map obtained on the linear domain as a final improvement result, such as formula **(3)**:

$$\underset{c\in\{R,G,B\}}{R^c}(x,y)=I(x,y)/\left[T(x,y)+\varepsilon\right] \tag{3}$$

where ε is a small constant to prevent the occurrence of a zero denominator. From formula **(3)**, it can be seen that when the value of the estimated illumination map T is less than the original map I, the reflection map is oversaturated(It means the gray values greater than 1), and an over-exposure will take place.

2.2Preliminary Illumination Estimation and Optimization

To keep the reflection map accurate (reflectivity greater than 1), the maximum of the three channels of the color of each pixel in the original image is used as the initial illumination estimation component. It is obtained in equation **(4)**:

$$T_{init}(x,y)=\max_{c\in\{R,G,B\}} I^c(x,y), \tag{4}$$

where T_{init} represents the initial component of the estimated illumination. Retinex theory assumes that the illumination component in the actual scene exists primarily in the low-frequency part of the image, and the change is moderate; In high-frequency parts of the image, such as edge textures, the reflection component is the majority [7]. Thus, the optimization method used in this paper is formula **(5)** [13] to preserve edge structure and smooth texture.

$$\min_L \left\|T-L\right\|_2^2+\lambda \lim_{\varepsilon\to 0^+}\sum_{d\in\{h,v\}}\frac{W_d(x)\left(\nabla_d L(x)\right)^2}{\left|\nabla_d T(x)\right|+\varepsilon}, \tag{5}$$

where the formula prefix $\left\|\cdot\right\|_2$ is the ℓ_2 norm, which is used to represent the similarity between the optimal illumination map and the original illumination map, and the postfix formula is used to represent the smoothness of the optimum illumination map. λ is the parameter used to equilibrate the ℓ_2 norm and ℓ_1 norm. T is the guided filtered illumination map, L is the illumination map after a structural priori optimization, and ∇T represents the first order central difference between the horizontal and vertical

directions of T . W is the matrix of weights, which is expressed as formula **(6)**:

$$W_d(x) = \sum_{y \in \omega(x)} \frac{G_\sigma(x, y)}{\left| \sum_{y \in \omega(x)} G_\sigma(x, y) \nabla_d T(x) \right| + \varepsilon}, \tag{6}$$

where the $\left| \nabla_d T(x) \right|$ is at a lower level in the window containing the texture so that the value of the item's value is primarily suppressed in this optimization problem, smoothing out the texture. $G_\sigma(x, y)$ represents the Gaussian kernel function with a standard deviation of δ , which can be expressed as formula **(7)**:

$$G_\sigma(x, y) = \frac{1}{2\pi\delta^2} \exp\left(-\frac{(x - x_0)^2 + (y - y_0)^2}{2\delta^2} \right) \tag{7}$$

where x_0 and y_0 are the window center coordinates. The larger the value of δ , the less impact of pixels around the specified pixel have on it, resulting in a larger weight value, smoother illumination, and more blurred edges. To balance structural consistency and smoothness, $\delta = 3$ was obtained in this paper and subsequent experiments [14].

2.3A Gamma Function Based on Brightness Average

In this subsection, a more detailed discussion of how the settings given for each parameter will cause a shift in image quality will be given in the Experiments and Analysis section.

The expression for the gamma function commonly used to adjust the brightness of the illumination map is shown in equation **(8)**:

$$V_{\text{out}} = a V_{in}^{\gamma}. \tag{8}$$

where V_{in} is the input image, V_{out} is the output image, a is the tuning parameter, γ is the gamma correction coefficient, and the larger the value of γ , the more jitter the transformation curve is observed.

Conventional gamma correction is difficult to deal with different conditions of mean value brightness. Thus our method introduces the tuning parameter b to non-linearize the coefficient γ to adapt to different illumination. The modified gamma function expression based on mean brightness adjustment is shown in equation **(9)**:

$$V_{out} = a V_{in}^{\frac{\gamma}{b}}, \tag{9}$$

combining the above considerations for gamma coefficients, the limit equation **(10)** is made while ensuring that the reflection map is not overexposed or underexposed:

$$0 \le \frac{\gamma}{b} \le 1, \tag{10}$$

Considering that the mean brightness can reflect the light situation, the expression of regulating parameter b is equation **(11)**:

$$b = (s + k)^E, \tag{11}$$

where k is a parameter used to fine-tune the deviation, E controls the slope of the transformation function, and s is a parameter that reflects the current pixel brightness and the mean brightness of the illumination map. Considering that the darker the overall image, the more information there is in the pixels of the low

brightness, the expression for s is equation **(12)**:

$$s = \left(\frac{256}{\mathrm{m}} \right) * (l - 1), \tag{12}$$

where m is the average brightness of the current illumination map and l is the brightness value that has been reduced to $[0,1]$. In the case of the same pixel brightness, when m tends to be low, the smaller the value of s, and therefore the larger the value of γ, and the lower the brightness of the low-light region of the illumination map, eventually the brightness of the reflection map in the corresponding region increases sufficiently.

To ensure that formula **(10)** holds, the value of k is as follows:

$$k = \gamma^{\frac{1}{E}} + \frac{256}{m}, \tag{13}$$

Combined with equations **(11) (12)** and **(13)**, equation **(13)** can be rewritten as formula **(9) (14)**

$$V_{out} = aV_{in}^{\frac{\gamma}{\left[\left(\frac{256}{m} \right) * (l-1) + (\gamma)^{\frac{1}{E}} + \frac{256}{m} \right]^{E}}}. \tag{14}$$

2.4 A Weighted Fusion Method According to the Gray Entropy

The original low-light image retains the original edge structure of the image. Considering that a lot of effective information is hidden under low-light conditions, in this paper, we proposed the following fusion methods to extract the hidden information better:

$$T_{final} = W \circ D + T, \tag{15}$$

where T_{final} denotes the fusion illumination map as the final result, W denotes the weighted matrix, T denotes the input illumination, and D denotes the detail layer D is obtained as follows:

$$D = I - I_{filter}, \tag{16}$$

where I_{filter} is the initial illumination image after Gaussian filtering. To preserve as much of the edge structure as possible, the weighting matrix W is obtained as follows:

$$W_{\mathrm{i}} = 1 - \exp(\Delta Ent), \tag{17}$$

where ΔEnt is the difference between the gray entropy of the optimized illumination map and the original one. The gray entropy is only related to the gray probability, which can produce a broad response to very low-contrast textured structures and areas in low-light environments. The gray entropy can be expressed in the form of equation **(18)**:

$$Ent = -\sum_{i \in \omega(x)} rel(i) * \log_2 rel(i), \tag{18}$$

Gray entropy is not only related to the image but also to the selected window size. For further experiments, the size of the gray entropy window is set to 5.

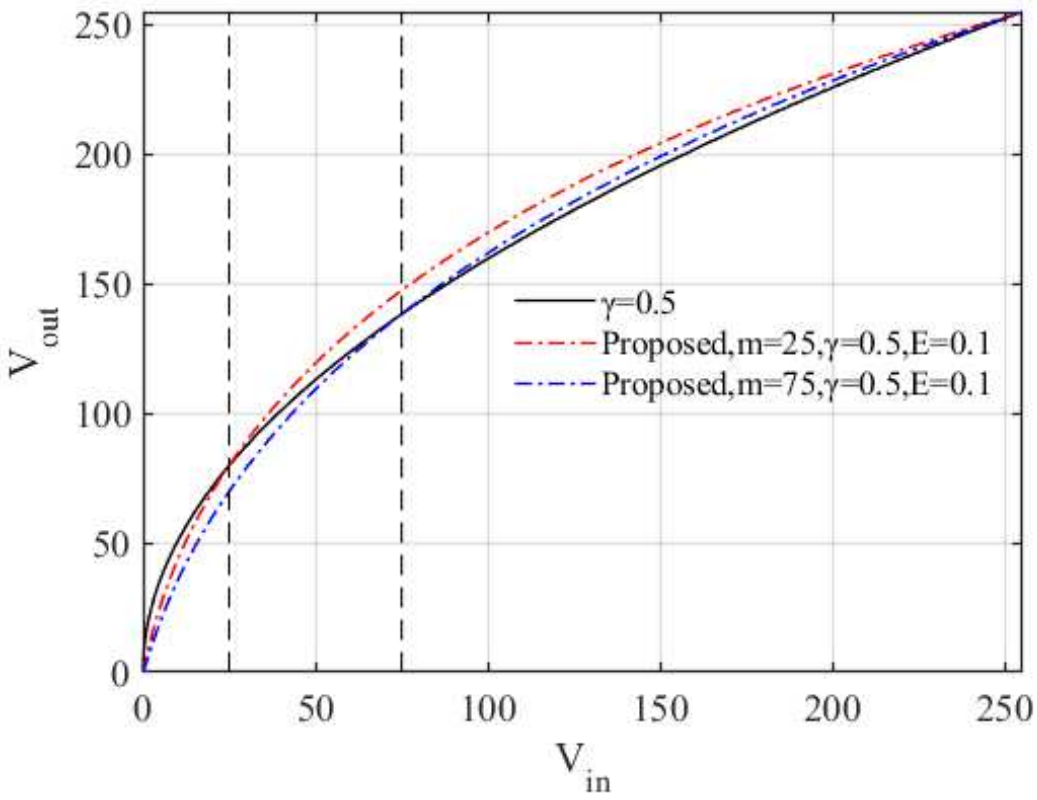
3. Experiments and Analysis

In this section, we first observe and discuss the difference caused by different parameter settings of the algorithm and give the parameter settings of this paper. Next, we introduce the experimental configuration and

compare the improved method with various advanced algorithms on subjective and objective indices (AG and EI) in representative low-light images.

3.1Parameters of the Gamma Function Based on Brightness Average

In order to further show the changes brought about by the equation **(14)** images with $b>1$ and $b>1$ are used as examples. After adjustment to equation **(8)**, as shown in Fig. 2, $b>1$ can be observed when the brightness of illumination map pixels is near to and below the average. As a result, when γ takes the same value after equation **(14)** processing, the brightness of the pixels mentioned above is lifted less than after formula **(8)** processing, resulting in better exposure of the reflection map. If the brightness of the pixels is in the range of more notable than the average value, the increase in brightness is more significant so that the reflection image will not be over-exposure.



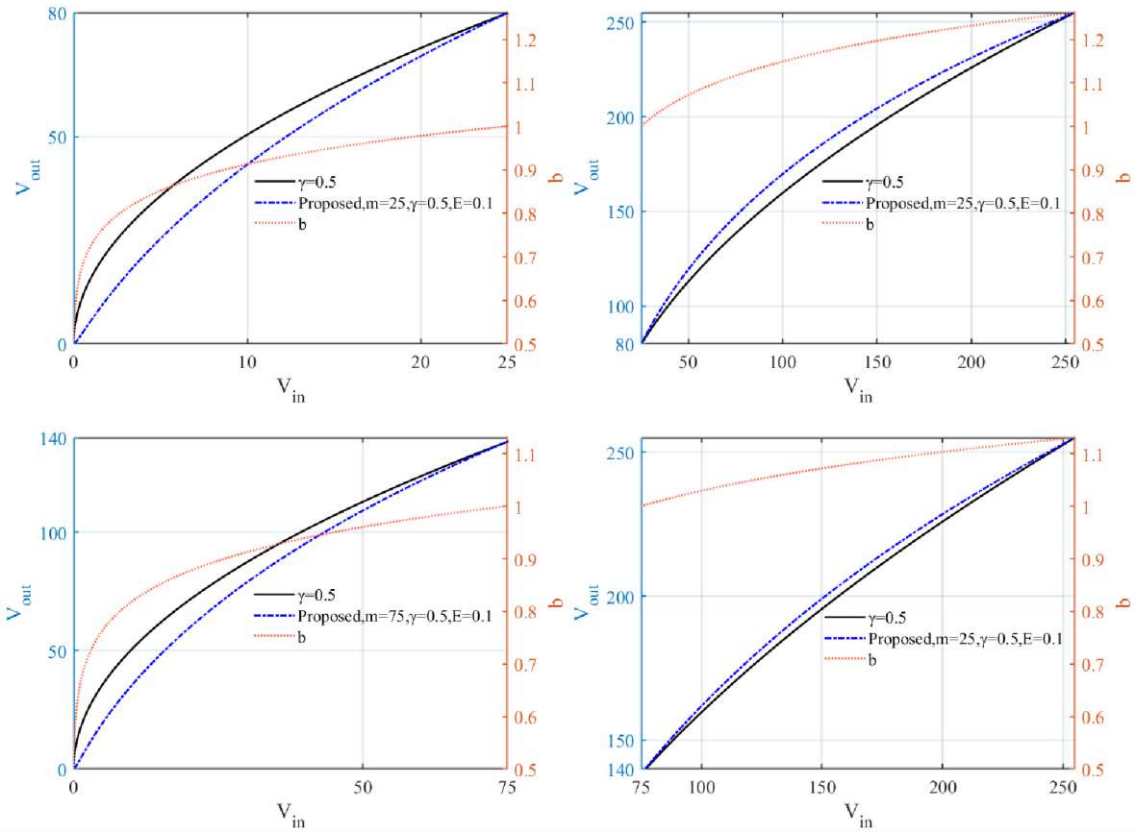
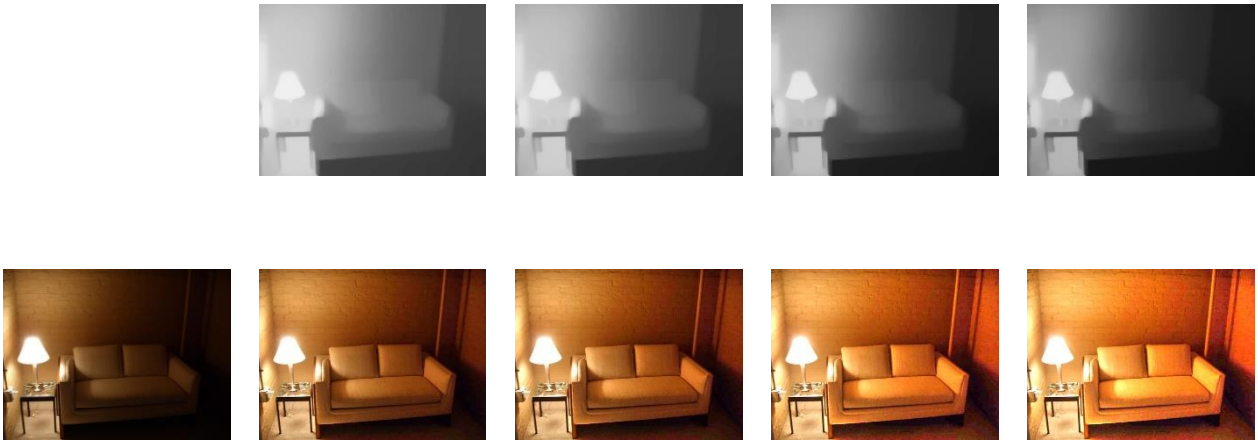


Fig. 2. Gamma function comparison graph..

The parameter γ in equation **(8)** affects the curvature of the curve and has a large influence on the effect of the image enhancement. This paper discusses the enhancement effect of γ on the image. From Fig. 3 and Fig. 4, we see the difference of the illumination and enhanced images with γ equal to 0.5,0.6,0.8, and 1 in two different scenes.

In order to further evaluate the parameter settings, the paper introduces quality assessment metrics based on the peak signal-to-noise ratio (PSNR), structural similarity index (SSIM) , average gradient (AG) and edge intensity (EI). **Table 1** and **Table 2** show how the quality assessment metrics change as the γ is varied.

As γ gets larger, the overall brightness of the image increases.At the same time, the rise in γ also leads to a gradual decrease in PSNR and SSIM values, and a gradual increase in AG and EI .This means that the quality of the image and the richness of the texture details are improved, but it is also accompanied by an increase in the degree of distortion. Therefore, In the subsequent experiments, all γ is fixed to 0.8. This ensures good brightness enhancement of the image without over-exposure.



(a)Original image (b) $\gamma = 0.5$ (c) $\gamma = 0.6$ (d) $\gamma = 0.8$ (e) $\gamma = 1$

Fig. 3. Visual comparison of illumination and enhanced images with different parameters γ in scene Ⅰ. From (b)to (e):Effect of parameter γ by setting γ to 0.5,0.6,0.8 and 1 respectively with fixed $E = 0.1$.



(a)Original image (b) $\gamma = 0.5$ (c) $\gamma = 0.6$ (d) $\gamma = 0.8$ (e) $\gamma = 1$

Fig. 4. Visual comparison of illumination and enhanced images with different parameters γ in scene Ⅱ. From (b)to (e):Effect of parameter γ by setting γ to 0.5,0.6,0.8 and 1 respectively with fixed $E = 0.1$.

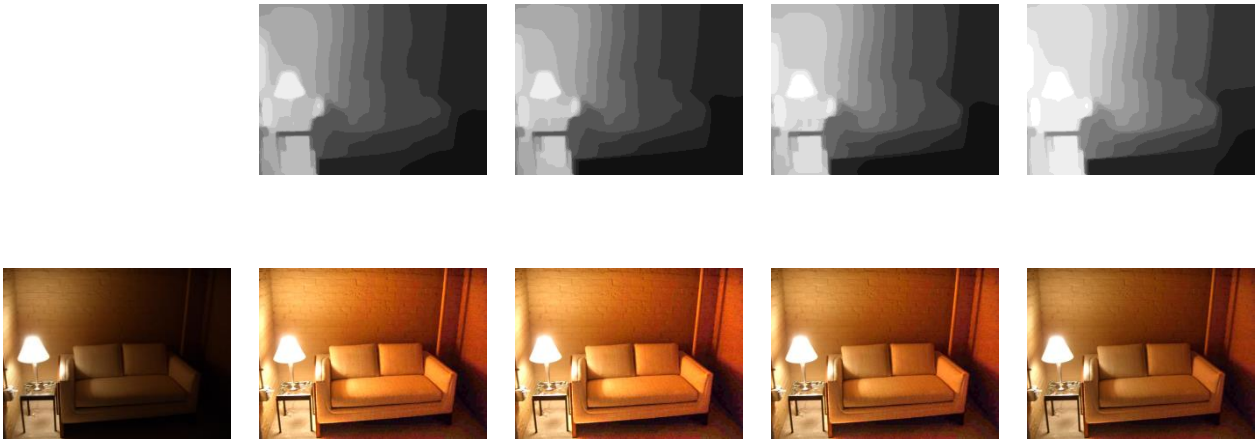
Table 1: Quality assessment metrics in enhanced image to compare γ of different sizes in scene Ⅰ

Metrics	$\gamma = 0.5$	$\gamma = 0.6$	$\gamma = 0.8$	$\gamma = 1$
PSNR	15.598	12.795	8.035	5.090
SSIM	0.363	0.255	0.133	0.094
AG	4.774	5.111	5.766	5.923
EI	18.786	23.048	31.918	36.350

Table 2: Quality assessment metrics in enhanced image to compare γ of different sizes in scene II

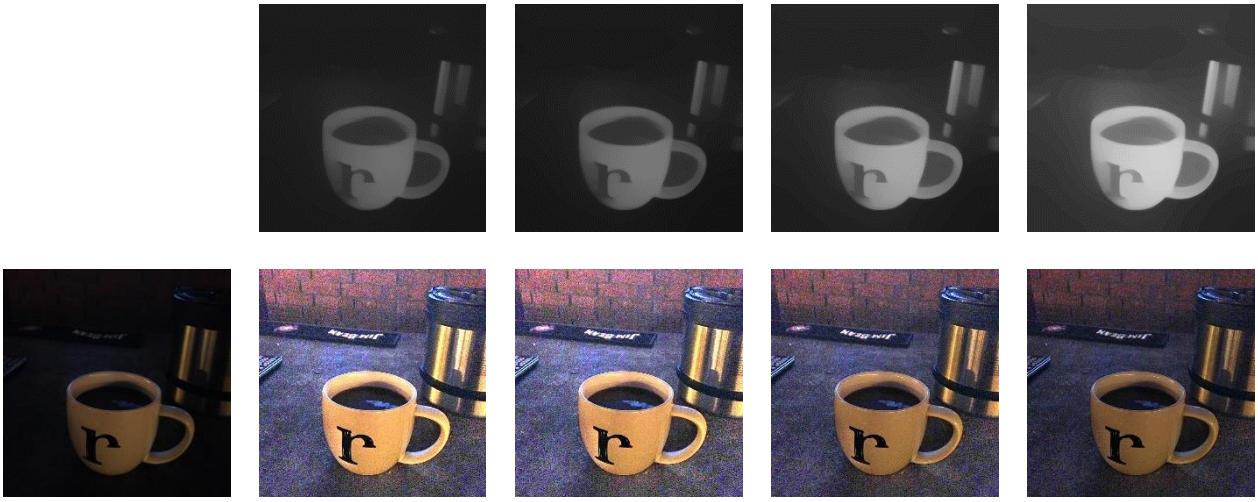
Metrics	$\gamma = 0.5$	$\gamma = 0.6$	$\gamma = 0.8$	$\gamma = 1$
PSNR	16.901	14.558	10.778	8.909
SSIM	0.616	0.534	0.421	0.373
AG	3.570	3.986	4.860	5.264
EI	36.427	40.593	49.332	53.325

In the nonlinear adjusting Gamma function proposed in this paper, the value of parameter E determines the degree of closeness between the transform function and the gamma function **(8)**. If the value of E is large, the light enhancement effect is weak in the low-light region and good robust in the high-light region. It results in a limited light enhancement in the reflection image. Conversely, when E is small, the reflection is more likely to have over-exposure. To optimize the parameters, several experiments were conducted as shown in Fig. 5 、 Fig. 6 、 **Table 3** and **Table 4**.



(a)Original image (b) $E = 0.01$ (c) $E = 0.1$ (d) $E = 0.5$ (e) $E = 1$

Fig. 5. Visual comparison of illumination and enhanced images with different parameters E in scene Ⅰ. From (b)to (e):Effect of parameter E by setting E to 10^{-2},0.1,0.5 and 1 respectively with fixed $\gamma = 0.8$.



(a)Original image (b) $E=0.01$ (c) $E=0.1$ (d) $E=0.5$ (e) $E=1$

Fig. 6. Visual comparison of illumination and enhanced images with different parameters E in scene II. From (b)to (e):Effect of parameter E by setting E to 10^{-2},0.1,0.5 and 1 respectively with fixed $\gamma=0.8$.

Table 3: Quality assessment metrics in enhanced image to compare E of different sizes in scene I

Metrics	$E=0.01$	$E=0.1$	$E=0.5$	$E=1$
PSNR	8.102	7.977	11.475	16.040
SSIM	0.123	0.126	0.216	0.358
AG	13.767	14.342	10.630	7.234
EI	126.408	131.521	97.578	66.448

Table 4: Quality assessment metrics in enhanced image to compare E of different sizes in scene II

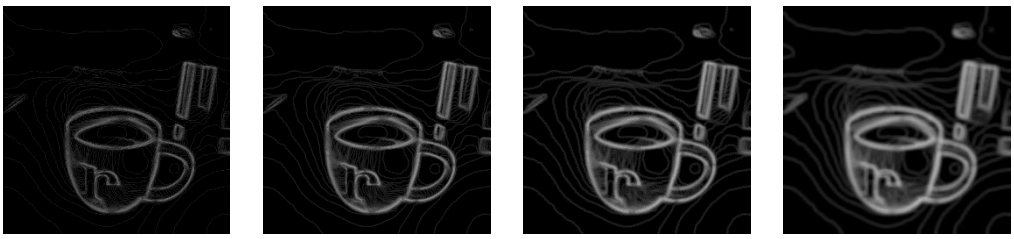
Metrics	$E=0.01$	$E=0.1$	$E=0.5$	$E=1$
PSNR	11.163	10.778	12.915	16.095
SSIM	0.429	0.421	0.487	0.576
AG	4.673	4.860	4.409	3.772
EI	47.457	49.332	44.836	38.438

If $E=0.01$, the reflection map is high on average brightness, but an overexposure problem exists at edges, such as the mouth of a coffee cup. However, if $E=0.5$ or $E=1.0$, a lack of brightness enhancement is observed in the enhanced map.Although it changes less in the structure of the original picture when E is gradually increased, it also means that its enhancement is lacking. This phenomenon can also be seen by observing the picture subjectively. Finally, E is chosen to be 0.1.

In the edge fusion method based on gray entropy, the value of the gray entropy is related to the image and

the window size setting. As the window size increases, the dynamic range of the grayscale entropy increases too. While this is a more accurate depiction of grayscale changes, it is also easier to capture false edges.

We extend the range of gray entropy to $[0, 255]$ for ease of observation. According to the results of several experiments, it is found that when the gray-scale entropy window size is selected as 3, the image edges are not observable. If the size is selected above 9, a large number of false edges appear. Finally, the size is selected as 5, as shown in Fig. 7:



(a) (b) (c) (d)

Fig. 7. Gray entropy map of different windows.

3.2 Experimental Conditions and Algorithmic Parameters

It has been a challenging task to enhance images captured under extremely poor lighting conditions without causing overexposure, halo effect or color distortion. In order to verify the robustness of the proposed method, four images representing different low-light scenes: the Coffee Cup, Sofa, Boat, and Cliff were selected for experiments. The Coffee Cup and Boat images reflect the low-light phenomenon caused by insufficient light sources indoors and outdoors. In contrast, the Sofa and Cliff plots reflect the low-light phenomenon due to backlighting indoors and outdoors. Test images are taken from the dataset provided by Loh et al. [24] and Guo et al. [13]. The proposed method was also compared to the other six advanced algorithms in terms of subjectivity and objectivity, respectively: The Control Limited Adaptive histogram equalization (CLAHE) [6], gamma correction(GC), MSR [9], SRIE [22], RetinexNet [17] and LightenNet [21]methods.

To ensure fairness, the parameters of all algorithms were adjusted to the optimum. The closer γ is to 1 in GC parameters, the worse the image enhancement. So we set the parameter to $a = 1$ and $\gamma = 0.5$; MSR [9] Gaussian scale constant is set to 15, 80, 200; The SRIE [22] model also has a gamma correction process. To avoid over-exposure of the enhancement map, γ was adjusted to 0.6; In the RetinexNet [17] method, the low-light dataset was chosen from [17] for training.

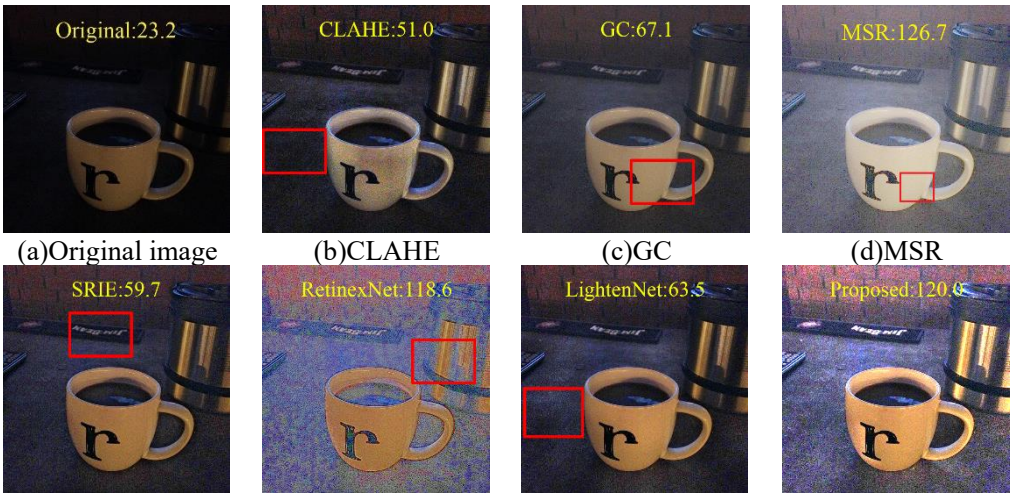
The hardware platform used in the experiment is the Intel (R) Core (TM) i7-8700 CPU, 3.20GHz CPU, and Windows 10 operating system with 32GB of memory. The parameters of the algorithm are given as follows:

Table 5: Experimental parameter settings

Algorithm	Parameters
CLAHE	We set the grayscale range to $[0, 255]$.
GC	$a = 1, \gamma = 0.5$.
MSR	We set the three Gaussian scale constants to 15， 80， 200.
SRIE	We set the error parameter to 0.01 and $\gamma = 0.6$.
RetinexNet	We choose the original dataset for 100 training iterations. Up to 16 images can be trained simultaneously in each round.
LightenNet	$\gamma = 1.7, n_1 = 32, n_2 = 16, n_3 = 8, n_4 = 1$
Proposed	$a = 1, E = 0.1$， $\gamma = 0.8$， The grayscale entropy window size is 5.

3.2Subjective Assessment

In each image, the yellow font indicates the global average brightness to partially reflect the enhancement effect. Fig. 8 shows the Coffee Cup image with inadequate light source and many details were submerged in the darkness (e.g., the blanket in the back and the thermos on the right). As can be seen in the red box in Fig. 8 (b), due to the low overall contrast ratio, CLAHE cannot effectively enhance the image; GC and MSR algorithms can boost brightness areas to some extent, but they have limited color recovery, as shown in Fig. 8 (c) (d) for coloring on coffee cups; As can be seen from Fig. 8 (e), the SRIE recovered well in color, but the improvement in brightness is weak, such as the coverage in the red box; Fig. 8 (f) shows that the recovered RetinexNet leads to serious noise in restored images, such as thermos cups in red boxes; LightenNet method is less effective in enhancing low-light areas, as shown in the Fig. 8 (g). Our method can effectively improve the brightness and contrast of low-light regions, retain more detail, and make the visual effect more user-friendly.



(a)Original image (b)CLAHE (c)GC (d)MSR

(e)SRIE (f) RetinexNet (g) LightenNet (h)Proposed

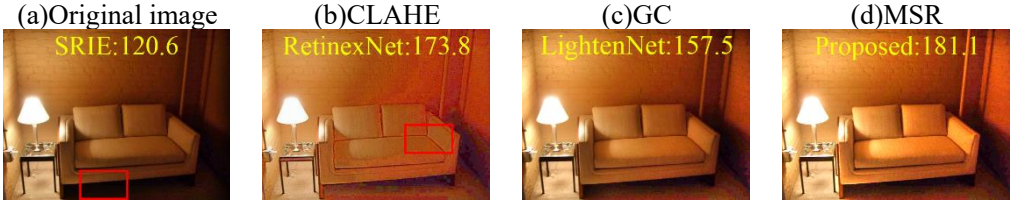
Fig. 8. Coffee Cup.

Fig. 9 shows the image of Sofa with uneven low light in the room. The light from the table lamp on the left and the sofa on the right caused backlighting, which created a distinct low-light area. The CLAHE algorithm, though, optimizes the processing of each image block and limits contrast. However, It is characterized by a

frequency calculation based on pixel values. This resulted in a slight recovery of the enhancement map in the structurally low-light regions, as shown in Fig. 9 (b) in the red box region; GC has a local overexposure, as shown in Fig. 9 (c) in the red box of the base area of the lamp; After MSR algorithm processing, severe overexposure appears, such as the wall area in Fig. 9 (d). The SRIE algorithm improves global brightness without distortion, but there is a problem of limited brightness improvement in low-light regions, as the region below the sofa in Fig. 9 (e); The image processed by the RetinexNet algorithm has a color chip problem, as shown in Fig. 9 (f) on the right side of the sofa; The LightenNet algorithm enhances well, as does the proposed method ,which can effectively enhance the brightness of dark light regions and has high contrast and a better processing effect.



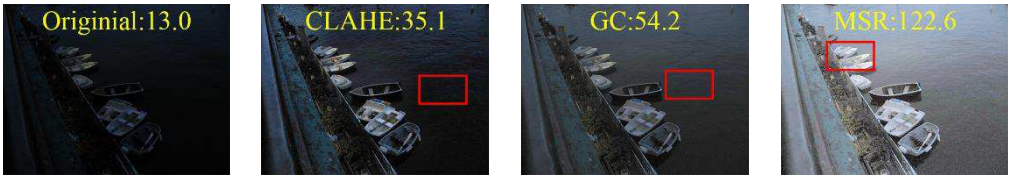
(a)Original image (b)CLAHE (c)GC (d)MSR



(e)SRIE (f) RetinexNet (g) LightenNet (h)Proposed

Fig. 9. Sofa.

Fig. 10 shows the Boat image with outdoor low light. Piers and ships have plenty of detail but are buried by low light. CLAHE and GC, while having a certain image quality, have limited recovery for dark light regions, such as the lake area in Fig. 10 (b) (c); By observing Fig. 10 (d), the MSR model is prone to exposure of the restored image, such as a ship with its lights on. SRIE improves the image's visual quality, but the vegetation in Fig. 10 (e) shows limited contrast improvement in the dark area. RetinexNet does a great job of brightening up images, but the steps need to be more natural in color. LightenNet has poor enhancement at the edges of the image structure, and the overall brightness improvement is not high. In contrast, the low-light region of the proposed algorithm recovers well and does not produce an overexposure phenomenon.



(a)Original image (b)CLAHE (c)GC (d)MSR

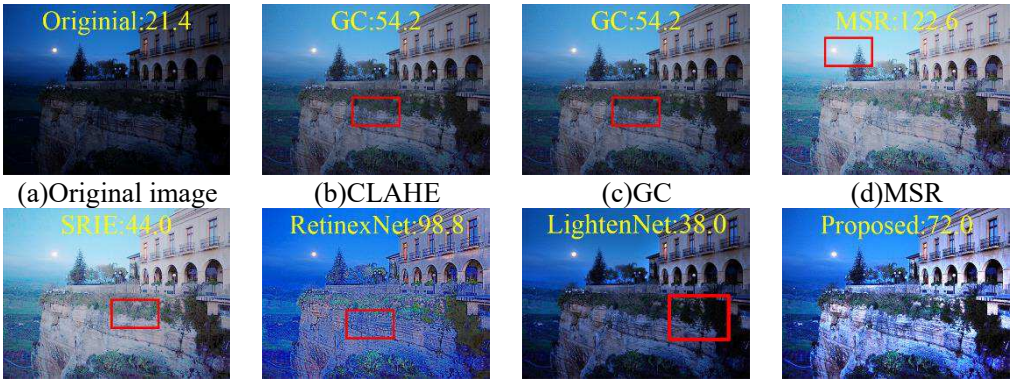


(e)SRIE (f) RetinexNet (g) LightenNet (h)Proposed

Fig. 10. Boat.

Fig. 11 Cliff is outside with low, uneven light. Locally low light occurs in the sky areas and cliff walls due to uneven light distribution. As can be seen from the clouds and trees in Fig. 11 (b), the problem of the enhancement of the dark regions occurs after CLAHE treatment; the GC algorithm still has the problem of not effectively enhancing the contrast of low-light regions, as shown in Fig. 11 (c), where the cliffs meet the rocks. MSR restored global brightness better, but a halo of light appeared on the edges, as seen in the branches next to the moon in Fig. 11 (d). When SRIE processed the image, color saturation remained low, and some areas blurred. It can be seen at the junction of vegetation and rocks at the cliff's edge in Fig. 11 (e); RetinexNet does a better job of brightening images. However, there are problems with halo artifacts and color imbalances in the cliff-

wall areas in the red box in Fig. 11 (f). LightenNet's overall brightness improvement is not high, and details are lost in dark areas. Our algorithm can keep the image details of the low-light region of the original image well, and no exposure can coincide.



(a)Original image (b)CLAHE (c)GC (d)MSR

(e)SRIE (f) RetinexNet (g) LightenNet (h)Proposed

Fig. 11. Cliff.

3.3 Objective Assessment

The proposed algorithm is designed to restore brightness and contrast in low-brightness regions. In this paper, we adopted the blind image quality assessment commonly used in objective data. These were Average Gradient (AG) and Edge Intensity (EI), respectively. The AG equation is as follows:

$$AG = \frac{1}{(M-1)(N-1)} \sum_{i=1}^{M-1} \sum_{j=1}^{N-1} \sqrt{\frac{\left(I(i+1,j)-I(i,j)\right)^2 + \left(I(i,j+1)-I(i,j)\right)^2}{2}}, \tag{23}$$

where M , N are the widths and heights of the image, and I is the pixel value of the image. AG measures the image detail. The larger the AG value, the more and clearer the image detail. The EI term is:

$$EI = \frac{\sqrt{\sum_{i=1}^{M} \sum_{j=1}^{N} s_x(i,j)^2 + s_y(i,j)^2}}{M * N}, \tag{24}$$
$$s_x = F * h_x, s_y = F * h_y,$$

Where h_x and h_y are Sobel operators in the x-and y-directions. s_x and s_y are the outcomes after the convolution of the Sobel operators. We use EI to measure the sharpness of the structure of the image. The larger the value, the more evident the edges of the structural texture are.

As shown in **Table 6** and **Table 7**, our algorithm's AG and EI indices are significantly improved compared to the low-light image in different conditions. It is also superior to most other algorithms. The above phenomenon shows that the detail and texture of the enhanced image processed by the proposed method are better than others. In Fig. 9, the AG index of the CLAHE method is slightly superior to that of this paper. Although this method overhandles the edge of the block and block, there is still color distortion, and the overall brightness could be higher. In contrast, the proposed algorithm enhances the color and brightness of the image. We note that the RetinexNet algorithm is second only to ours. However, subjective assessments of Fig. 10 to Fig. 11 show that images restored by Retinex-net have significant halation artifacts and color imbalances.

Table 6:AG comparison of test set images

Algorithm	CoffeeCup	Sofa	Boat	Cliff
The original image	2.222	2.246	1.180	3.410
CLAHE	6.532	**4.894**	3.552	9.724
GC	4.479	2.956	2.500	5.796
AGC	2.131	2.658	1.262	4.288
MSR	6.477	3.536	4.304	7.670
SRIE	6.351	3.032	3.549	6.072
RetinexNet	14.131	4.446	6.967	10.013
Proposed	**14.348**	4.861	**8.366**	**13.216**

Table 7: EI comparison of test set images

Algorithm	CoffeeCup	Sofa	Boat	Cliff
The original image	20.554	23.132	12.174	32.652
CLAHE	59.645	49.255	36.492	92.492
GC	41.337	30.019	25.568	54.961
AGC	19.866	27.126	13.046	40.892
MSR	59.590	35.409	43.711	72.150
SRIE	58.911	31.458	36.534	58.493
RetinexNet	126.799	44.672	69.225	113.905
Proposed	**131.576**	**49.333**	**85.518**	**125.434**

By comprehensively comparing subjective and objective assessments, the proposed algorithm shows good performance in every performance index. It is more robust and has clear advantages over the compared methods. While the proposed algorithm may not be the highest regarding the individual objective indicators, the enhanced image is significantly improved and within normal limits compared to the original plot. When combined with subjective vision, the low luminance region of the image is significantly increased by this method. In addition, the image details have been fully retained, without features such as color distortion.

4. Conclusion

Based on the Retinex model, this paper proposes a photogram correction method. It is based on the weighted fusion of the gamma function and gray entropy with mean light curve fitting. In addition, the improved Retinex algorithm was adopted to improve the brightness and contrast of the low-light images. As an initial illumination estimation component, the maximum of the three color channels of each pixel was obtained in the

original pattern. Then the illumination map is optimized using the priori structural optimization problem. A gamma function based on the brightness average is adopted to correct the image. Finally, the difference in gray entropy is taken as the weight, and the detail layer is weighted and fused into the corrected illumination pattern to enrich the detail of the image. The algorithm performs well in brightness enhancement and AG and EI objective indicators. On the Coffe Cup, the Average Gradient reaches up to 14.38, and the Edge Intensity reaches up to 131.576, which is a great improvement compared to the original image. The proposed method outperforms the other 7 methods in both subjective and objective assessments. The research in this paper helps improve the performance of machine vision technology applications, such as fault detection, feature matching, and target tracking.

Disclosures

The authors declare no conflicts of interest.

Acknowledgments

This work was supported in part by the Key Research and Development Program of Zhejiang Province under Grant 2022C01139 , and in part by the Key Research and Development Program of Jinhua. This research was partly supported by Zhejiang Provincial Natural Science Foundation of China under Grant No. LTGC23F030001. This work was also supported by the National University Students Science and Technology Innovation Project (CN) under Grant 202110345038.

Reference

[1]Wang W, Chen Z, Yuan X, et al. Adaptive image enhancement method for correcting low-illumination images[J]. Information Sciences, 2019, 496: 25–41.

[2]Jahidul I M, Youya X, Junaed S. Fast Underwater Image Enhancement for Improved Visual Perception[J]. IEEE Robotics and Automation Letters, 2020, 5(2): 3227–3234.

[3]Yuhui M, Jiang L, Yonghuai L, et al. Structure and Illumination Constrained GAN for Medical Image Enhancement[J]. IEEE Transactions on Medical Imaging, 2021, 40(12): 3955–3967.

[4]Shengwen F, Zhanjun J. Research on Image-Based Detection and Recognition Technologies for Cracks on Rail Surface[J]. 2019 International Conference on Robots & Intelligent System (ICRIS), 2019: 98–101.

[5]Kumar B A, Pankaj K, Shubham M. Salp Swarm Algorithm-Based Optimally Weighted Histogram Framework for Image Enhancement[J]. IEEE Transactions on Instrumentation and Measurement, 2020, 69(9): 6807–6815.

[6]Syamily A, R. D P, A. B A, et al. Algorithm for Underwater Cable Tracking Using CLAHE based Enhancement[J]. 2019 International Symposium on Ocean Technology (SYMPOL), 2019: 129–137.

[7]LAND， EDWIN H. The retinex theory of color vision [J]. Scientific American，1977,237 (6):108-128.

[8]Jingchun Z, Dehuan Z, Peiyu Z, et al. Retinex-Based Laplacian Pyramid Method for Image Defogging[J]. IEEE Access, 2019, 7: 122459–122472.

[9]Xianming L, Deming Z, Rong C, et al. Depth Super-Resolution via Joint Color-Guided Internal and External Regularizations[J]. IEEE Transactions on Image Processing, 2019, 28(4): 1636–1645.

[10] Sanjay G, N. C K. Fast Bright-Pass Bilateral Filtering for Low-Light Enhancement[J]. 2019 IEEE International Conference on Image Processing (ICIP), 2019: 205–209.

[11] Yu G, Yuxu L, Wen L R, et al. Low-Light Image Enhancement With Regularized Illumination Optimization and Deep Noise Suppression[J]. IEEE Access, 2020, 8: 145297–145315.

[12] Zhuang F, Shijie H. Low-Light Image Enhancement by Refining Illumination Map with Self-Guided Filtering[J]. 2017 IEEE International Conference on Big Knowledge (ICBK), 2017: 183–187.

[13] Guo X, Li Y, Ling H. LIME: Low-Light Image Enhancement via Illumination Map Estimation[J]. IEEE Transactions on Image Processing, 2017, 26(2): 982–993.

[14] Zhang Q, Nie Y, Zheng W-S. Dual Illumination Estimation for Robust Exposure Correction[J]. Computer Vision and Pattern Recognition (cs.CV), 2019.

[15] Jun X, Yingkun H, Dongwei R, et al. STAR: A Structure and Texture Aware Retinex Model[J]. IEEE Transactions on Image Processing, 2020, 29: 5022–5037.

[16] Xu Y, Yang C, Sun B, et al. A novel multi-scale fusion framework for detail-preserving low-light image enhancement[J]. Information Sciences, 2021, 548: 378–397.

[17] Chen W, Wenjing W, Wenhan Y, et al. Deep retinex decomposition for low-light enhancement[J]. arXiv preprint arXiv:1808.04560, 2018.

[18] Yonghua Z, Jiawan Z, Xiaojie G. Kindling the Darkness: A Practical Low-Light Image Enhancer[C]. Proceedings of the 27th ACM International Conference on Multimedia. 2019: 1632–1640.

[19] Li Z, Wang Y, Zhang J. Low-light image enhancement with knowledge distillation[J]. Neurocomputing, 2022.

[20] Wang W, Yan D, Wu X, et al. Low-light image enhancement based on virtual exposure[J]. Signal Processing: Image Communication, 2023, 118: 117016.

[21] Li C, Guo J, Porikli F, et al. LightenNet: A Convolutional Neural Network for weakly illuminated image enhancement[J]. Pattern Recognition Letters, 2018, 104: 15–22.

[22] Xueyang F, Yinghao L, Delu Z, et al. A Probabilistic Method for Image Enhancement With Simultaneous Illumination and Reflectance Estimation[J]. IEEE Transactions on Image Processing, 2015, 24(12): 4965–4977.

[23] Li M, Liu J, Yang W, et al. Structure-Revealing Low-Light Image Enhancement Via Robust Retinex Model[J]. IEEE Transactions on Image Processing, 2018, 27(6): 2828–2841.

[24] Loh Y P, Chan C S. Getting to know low-light images with the Exclusively Dark dataset[J]. Computer Vision and Image Understanding, 2019, 178: 30–42.